

STEADY AND UNSTEADY INVESTIGATIONS OF SPOILER AND FLAP AERODYNAMICS
IN TWO DIMENSIONAL SUBSONIC FLOWS

M. COSTES, A. GRAVELLE and J.J. PHILIPPE
Office National d'Etudes et de Recherches Aéronautiques
BP 72 - 92322 Châtillon Cedex, France

S. VOGEL
MBB
Postfach 107845
2800 Bremen (Germany)

H. TRIEBSTEIN
DFVLR
Bunsenstrasse 10, 3400 Göttingen, Germany

Abstract

An experimental study has been performed in the ONERA F1 pressurized wind tunnel on a 1 m chord supercritical airfoil equipped with a spoiler and a flap in a two-dimensional flow. Both spoiler and flap can be steadily deflected simultaneously and one control surface can then be driven with a harmonic motion, a white noise motion, or a ramp motion for various rise times. Steady and unsteady pressures, lift and moment coefficients depend on Reynolds number, mean steady deflection and frequency. The interaction between the control surfaces is examined. Unsteady pressure time histories for ramp type motions for various rise times and initial deflections are also given. Finally, some comparisons are presented between a theoretical method developed at ONERA and the experimental data for a steady deflected spoiler.

I. Introduction

The development of Active Control Technology has involved a special interest in control surface unsteady aerodynamics. From the computational point of view, the numerical codes available for calculating unsteady aerodynamics have for a long time been linear methods. An important effort has been underway for about 10 years to develop more accurate codes. But most of these methods remain inviscid ones, and consequently, they are unable to calculate the viscous effects on the flap characteristics or the separated flow induced by a spoiler, even in steady flows.

These facts prove the necessity of evaluating the steady and unsteady performances of spoilers and flaps from experimental data. A common experimental study shared by ONERA, MBB and DFVLR has been carried out with a two-dimensional model equipped with a spoiler and a flap. The goals of this collaboration were to improve knowledge of the aerodynamic forces induced by the steady or unsteady deflection of spoilers and flaps, and to obtain accurate measurements necessary to validate the prediction codes that are being developed in both countries.

II. Test facilities and model

The model (ACTTA Wing) was tested in the ONERA low speed pressurized wind tunnel F1 in
Copyright © 1986 by ICAS and AIAA. All rights reserved.

the Le Fauga test center. Figure 1 shows this model between two walls erected in the test section in order to assure 2D tests.

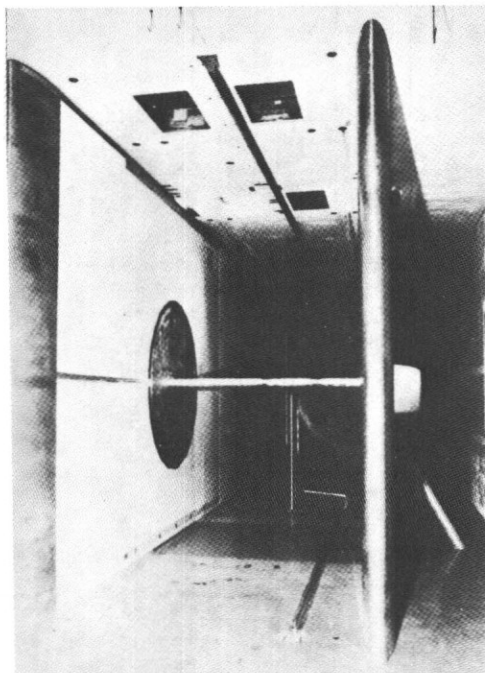


Figure 1. ACTTA Wing in F1 wind tunnel.

The ACTTA Wing (figure 2), manufactured by MBB, is a rectangular supercritical wing of 2 m span by 1 m chord. The three components are :

- the main box which can rotate around an axis located at 27.5% of the chord for angle of attack change ;
- the spoiler, 2 x 0.15 m, which can rotate from $\delta_{sp} = 0^\circ$ to $\delta_{sp} = 31^\circ$ around the hinge line located at 67% of the chord ;
- the flap, 2 x 0.125 m, which can move from $\delta_f = -5^\circ$ (upward) to $\delta_f = +10^\circ$ (downward) around its hinge line located at around 87.5% of the chord.

The model was equipped with 115 static pressure tapings along one middle and two lateral sections, 115 unsteady pressure pick-ups with the same chordwise distribution, 13

accelerometers and 4 strain gauge bridges. Angle of attack was fixed manually, whereas spoiler and flap were hydraulically actuated by a feedback servosystem. Static pressure measurements were processed by the F1 wind tunnel acquisition unit. The ONERA Structures Department was in charge of unsteady measurements. The acquisition equipment used is described in reference¹.

The test program included, for each control surface, the study of the following parameters for a harmonic excitation :

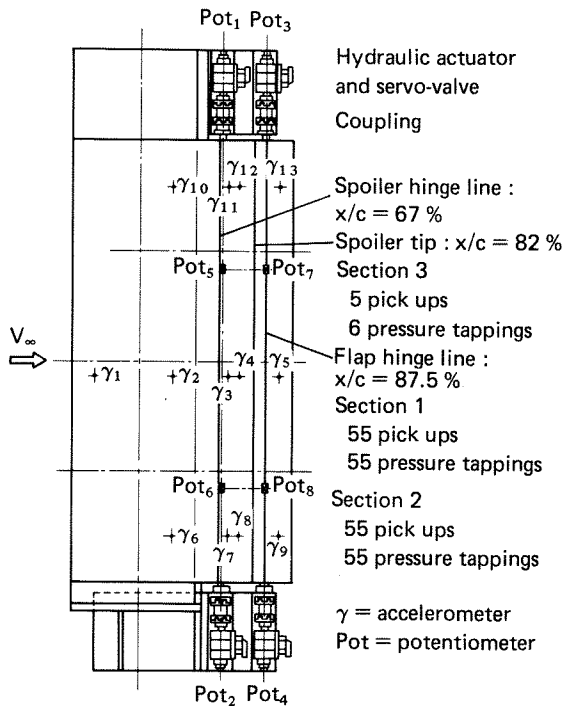


Figure 2. ACTTA Wing.

- mean deflection,
- oscillation amplitude,
- reduced frequency,
- Reynolds number.

Furthermore, the interaction between the two control surfaces has been examined (influence of a control surface static deflection on the other control efficiency). Finally, several white noise and "ramp" excitations were realized. The test program involved about 120 steady and 160 unsteady configurations. All the tests were performed at $M = 0.2$. The main configurations were systematically tested at a stagnation pressure equal to 1 bar corresponding to a Reynolds number of about 4 million, and at a stagnation pressure equal to 4 bars corresponding to a Reynolds number of about 16 million.

In this paper, we are mainly concerned with the influence of Reynolds number on control surface efficiency, the comparison between spoiler and flap characteristics, and the study of the interaction between control surfaces (spoiler and flap) in steady and unsteady configurations. Examples of the ramp

measurements are also given. Finally, we briefly present the computer code developed at ONERA to calculate the steady flow around an airfoil equipped with a spoiler, and some comparisons with experimental data are made.

III. Reynolds number effect

1) Steady configuration

Figure 3 shows the normal force evolution versus spoiler deflection calculated from the pressure integration for two Reynolds numbers (4 and 16 million) and for two flap angles. For $\delta_f = 5^\circ$, at low spoiler deflections, the normal force is greater at $Re = 16 \times 10^6$ than at $Re = 4 \times 10^6$. This is due to a better flap efficiency at high Reynolds numbers where viscous effects are less important, as proved by figure 4. On the other hand, for high spoiler deflections, the normal forces are lower at $Re = 16 \times 10^6$ than at $Re = 4 \times 10^6$, which shows that the spoiler efficiency is greater in this situation. The boundary layer thickness is lower on the spoiler and in front of it, and this may induce a greater effective spoiler angle.

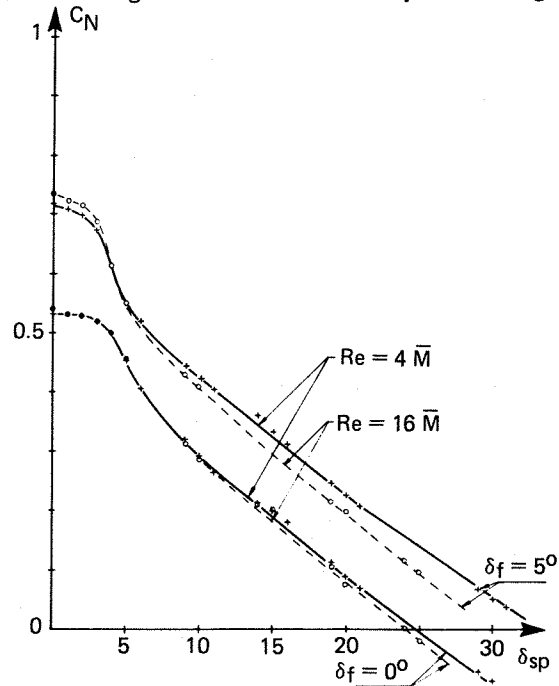


Figure 3. Airfoil with spoiler : steady Reynolds effect.

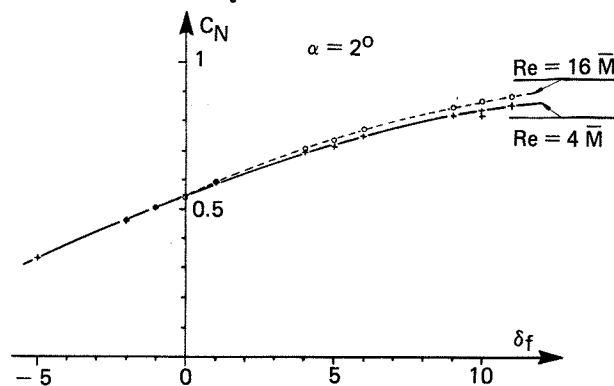


Figure 4. Airfoil with flap : steady Reynolds effect.

However, the conclusions on the Reynolds number influence may be erroneous because of its weakness and of the possible spoiler deformations which can appear when the stagnation pressure is increased.

2) Unsteady configurations

Figure 5 shows the Reynolds number effect on the spoiler efficiency. For small spoiler deflections ($\delta_{sp} = 3^\circ/5^\circ$), a noticeable evolution can be seen with a minimum for $Re \approx 13.5 \times 10^6$. For the two main Reynolds numbers tested (4.5×10^6 and 18×10^6), we obtain virtually the same results. Then, when the spoiler deflection is increased ($\delta_{sp} = 10^\circ$), this influence can no longer be detected: the reattachment point downstream of the spoiler is too far in the wake to have an effect on the unsteady lift. Finally, it must be noted that practically no effect can be seen on the phases.

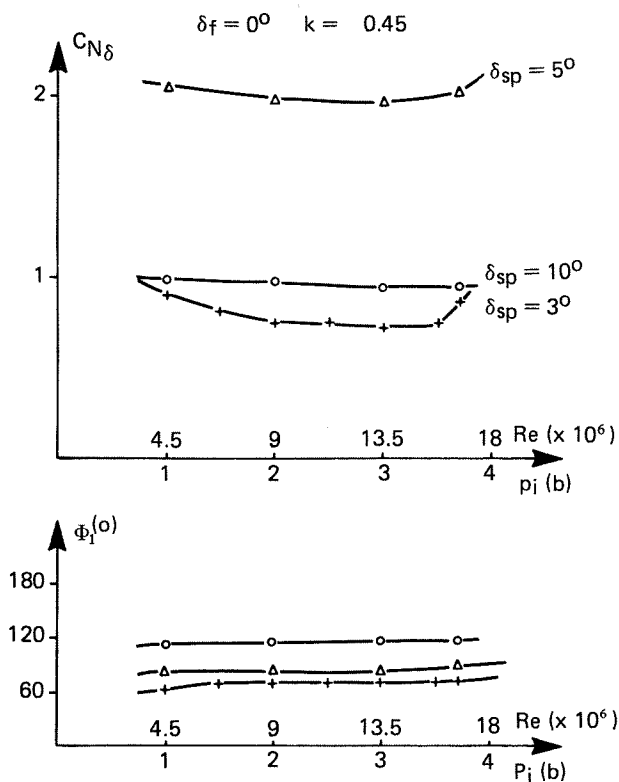


Figure 5. Oscillating spoiler : influence of Reynolds number on the lift coefficient.

For the flap, as illustrated on figure 6, the efficiency increases slowly with the Reynolds number, but this effect is very weak. This is in good agreement with steady measurements.

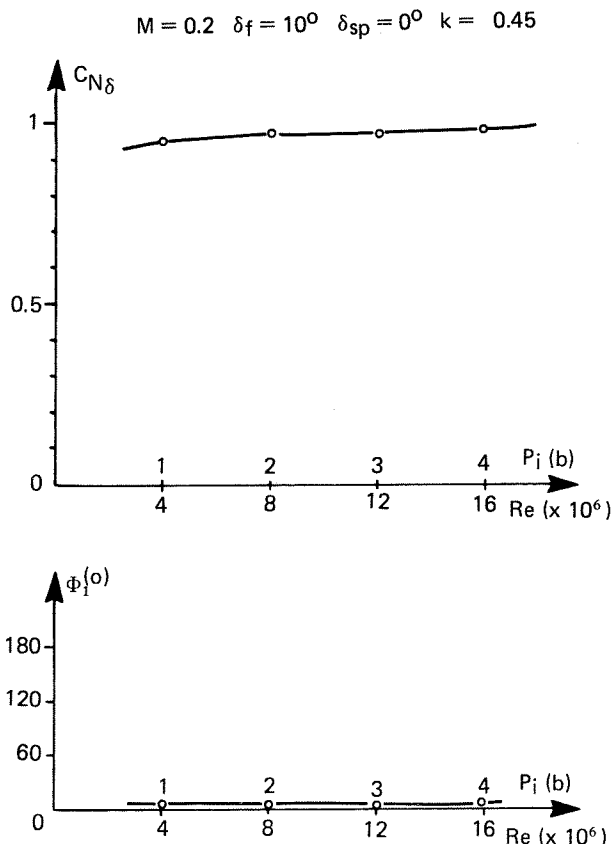


Figure 6. Oscillating flap : influence of Reynolds number on the lift coefficient.

IV. Comparison between spoiler and flap efficiencies

1) Influence of mean deflection

Figure 7 shows the unsteady pressures (first harmonic) measured on the airfoil for several spoiler deflections. The curve of the pressure distribution has a typical shape with the pressure evolution strongly depending on the mean deflection. The unsteady pressures generated by the spoiler motion are maximum for a spoiler angle of 5° , when the separated flow zone, induced by the spoiler, reaches the airfoil trailing edge. For a spoiler deflection greater than 10° , the unsteady pressure level remains quite constant. The phase evolution is more regular with a diminution of the phase lag with an increasing mean spoiler deflection.

The unsteady pressure distributions for the flap (figure 8) reveal a continuous decrease of the amplitudes and of the phase lag when the flap deflection increases. This is due to the occurrence of greater viscous effects, and more particularly, to the appearance of trailing edge separation which is obviously present at $\delta_f = 10^\circ$.

$M = 0.2 \quad \alpha = 2^\circ \quad F = 10 \text{ Hz} \quad \delta_f = 0^\circ \quad Re = 4 \bar{M}$

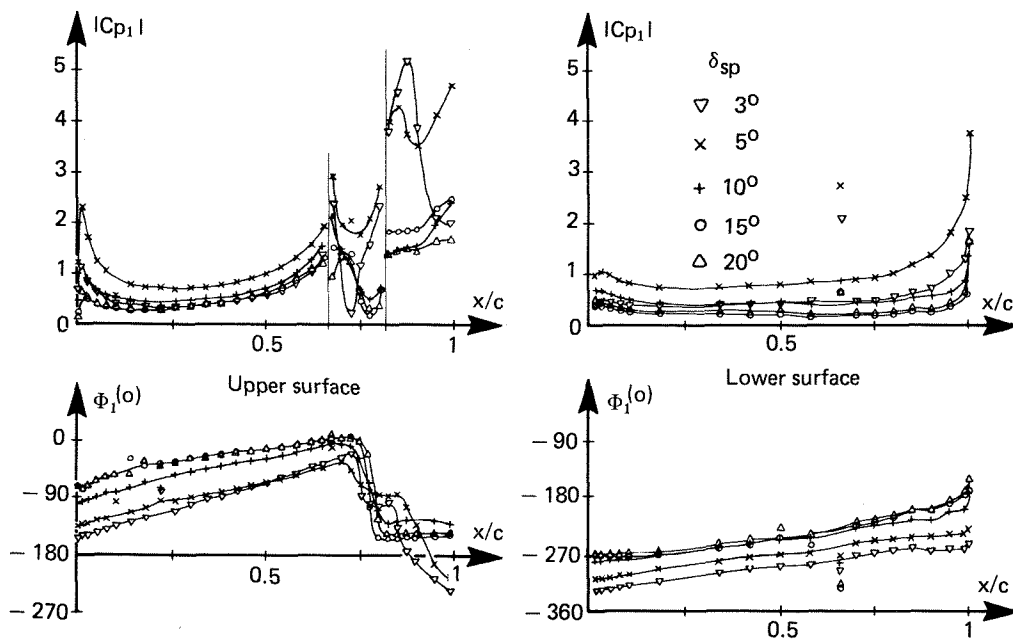


Figure 7. Oscillating spoiler : influence of spoiler deflection.

$M = 0.2 \quad \alpha = 2^\circ \quad \delta_{sp} = 0^\circ \quad Re = 4 \bar{M} \quad F = 10 \text{ Hz}$

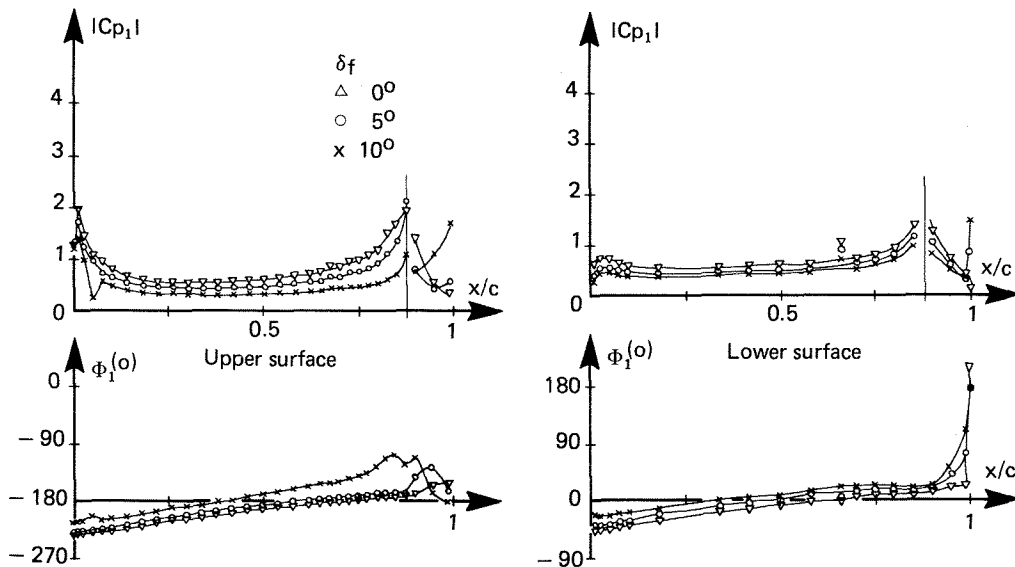


Figure 8. Oscillating flap : influence of flap deflection.

A comparison of the spoiler and flap efficiencies can be seen on figure 9. This efficiency is defined here as the unsteady lift capability (modulus of the first harmonic). As expected from the unsteady pressure distribution curves, the unsteady forces (C_N as well as C_M) present far less variations for the flap than for the spoiler at "low" steady deflections, and the phase lag is also generally much smaller for

the flap. A spoiler allows us to obtain high unsteady forces for small deflections and could be quite realistic for applications because small spoiler angles don't induce too severe a drag penalty. However, such good efficiency is obtained with quite large phase lags, the order of which is about 80° - 90° . Finally, it should be noted that the results on the modulus are in good agreement with steady results previously seen (figures 3 and 4).

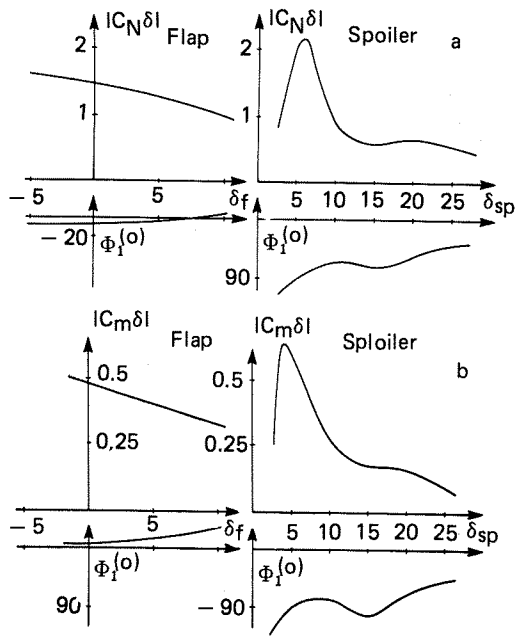


Figure 9. Comparison between spoiler and flap : influence of mean deflection.

2) Influence of the reduced frequency

For the same efficiency level for both the spoiler and the flap, figure 10 shows the influence of the reduced frequency on the lift coefficient. The flap unsteady lift increases slightly at high reduced frequencies and the spoiler efficiency strongly decreases with the frequency. In the region of greatest efficiency for each control surface (figure 11), the results are quite different ; for the flap, the lift coefficient decreases significantly with the frequency ; for the spoiler, the lift begins to decrease but, from $k \sim 0.5$, it increases regularly with the reduced frequency. Consequently, the effect of frequency strongly depends on the mean flow conditions.

$$M = 0.2 \quad Re_c = 16 \times 10^6$$

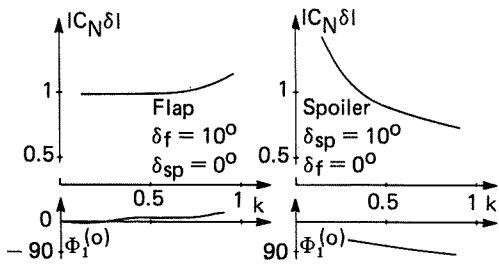


Figure 10. Comparison between spoiler and flap : influence of reduced frequency.

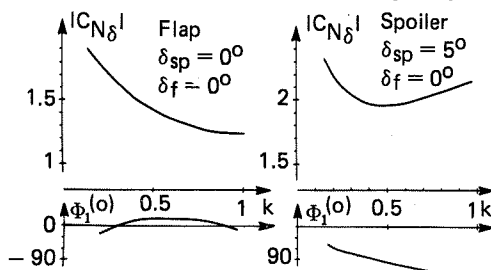


Figure 11. Comparison between spoiler and flap : influence of reduced frequency.

3) Aerodynamic interaction between control surfaces

a) Spoiler efficiency versus flap deflection

Figure 12 shows the spoiler steady efficiency curve for several flap deflections. The efficiency is defined as the lift loss capability given by the spoiler. The curve shape is quite classical with a non linear zone for small spoiler deflections where the control surface practically has no efficiency. This non linear zone is reduced as the flap angle is increased. For great spoiler deflections, the normal force curve slope doesn't depend on the flap deflection but the lift loss is obviously greater for high flap angles because the spoiler non linear zone is shorter. This phenomenon can be explained by looking at the airfoil pressure distribution (figures 13 and 14). For small spoiler deflections, the flow which is separated at the spoiler tip reattaches before the trailing edge, and the spoiler is only a local disturbance in the flow since no effect can be seen on the lower surface or on the upper surface in front of it (until $\delta_{sp} = 3^\circ$ on figure 13 and $\delta_{sp} = 6^\circ$ on figure 14). The spoiler deflection effect can be felt elsewhere only when the separated zone has reached the wake, inducing then a completely new pressure distribution and consequently a significant lift loss (from $\delta_{sp} = 7/8^\circ$ when $\delta_f = -5^\circ$ and from $\delta_{sp} = 4^\circ/5^\circ$ for $\delta_f = 5^\circ$).

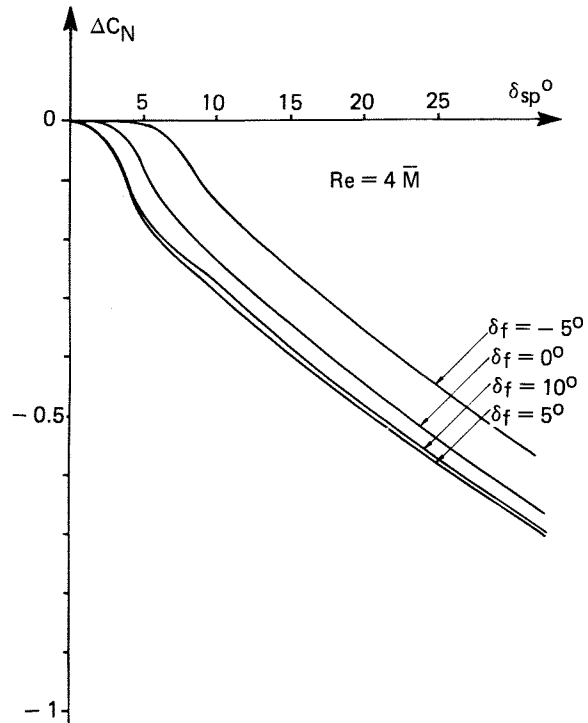


Figure 12. Influence of flap deflection on spoiler efficiency.

For the unsteady case, the same analysis can be done. For $\delta_{sp} = 3^\circ$ (figure 15), the influence of the flap deflection on the unsteady pressures is very important, with a pressure level decreasing when the flap deflection

decreases. On the other hand, for $\delta_{sp} = 20^\circ$ (figure 16), the unsteady pressures are exactly the same for all the flap deflections, except on the

lower side phases. Consequently we will have a constant unsteady lift capability which becomes obvious when looking at the steady curve given in figure 12.

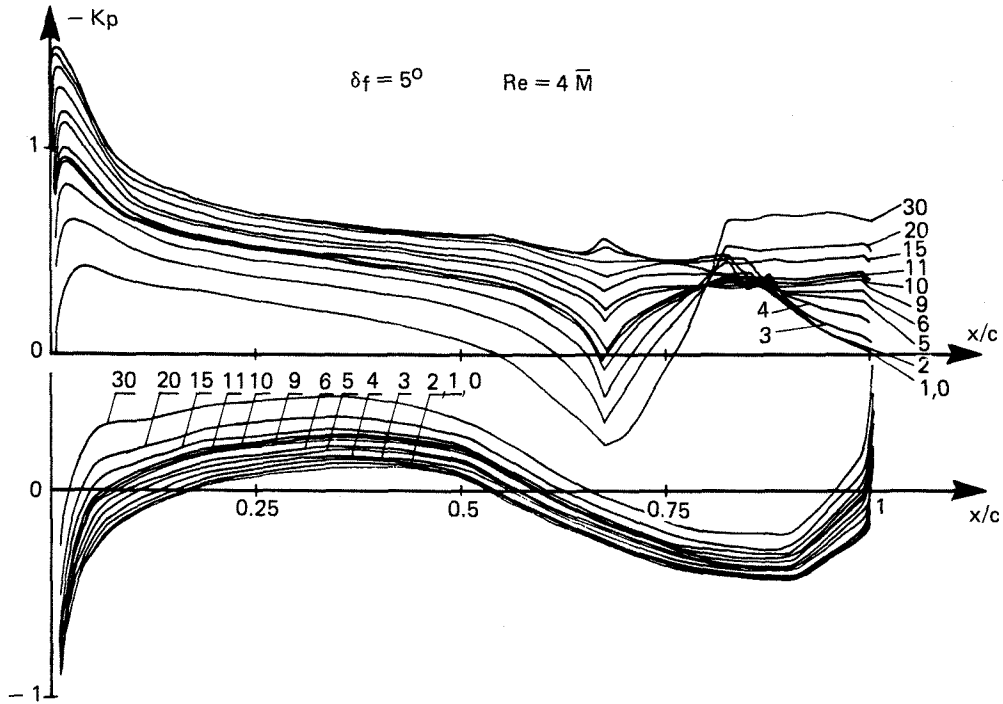


Figure 13. Steady pressure distributions versus spoiler deflection for 5° flap angle.

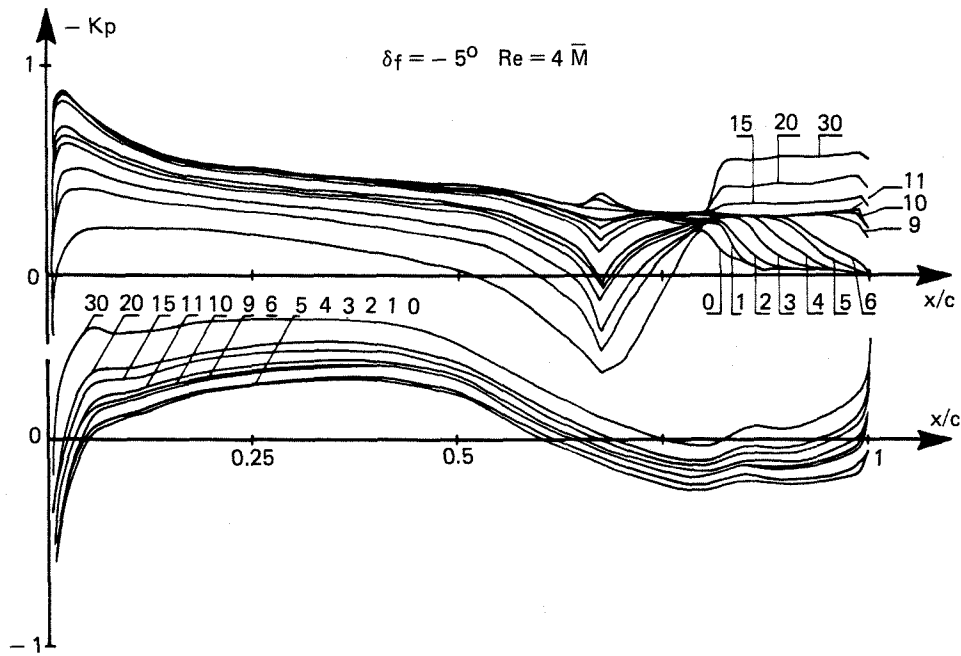


Figure 14. Steady pressure distributions versus spoiler deflection for -5° flap angle.

$M = 0.2 \quad \alpha = 2^\circ \quad \delta_{sp} = 3^\circ \quad F = 20 \text{ Hz} \quad k = 0.8976$

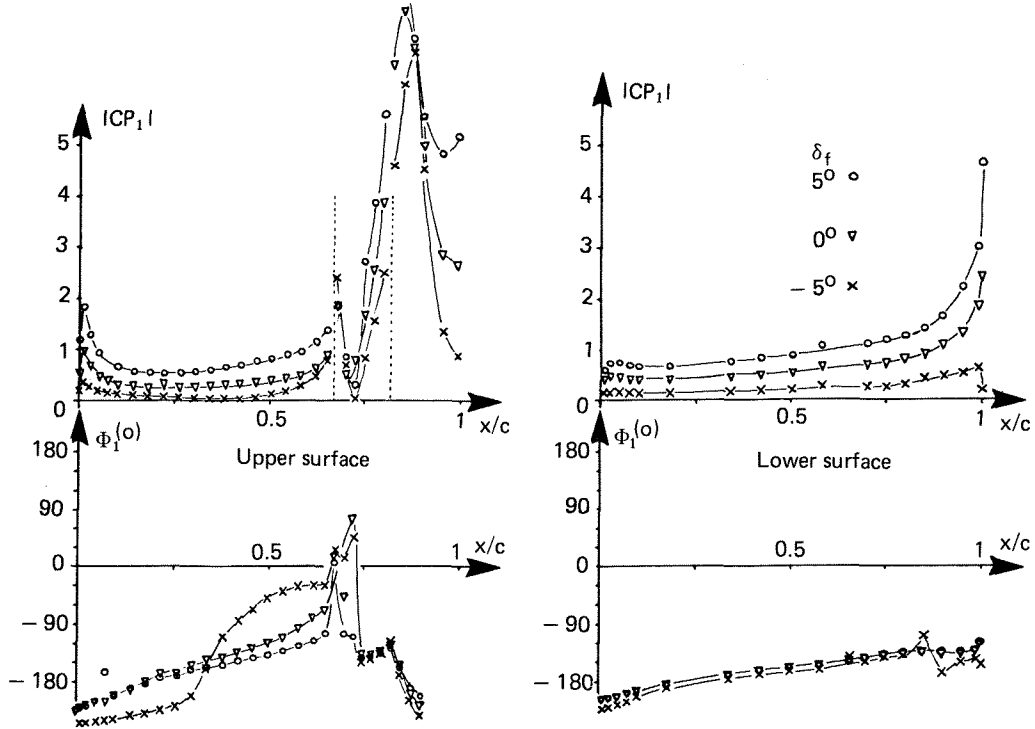


Figure 15. Oscillating spoiler : influence of flap deflection.

$M = 0.2 \quad \alpha = 2^\circ \quad \delta_{sp} = 20^\circ \quad F = 20 \text{ Hz} \quad k = 0.8976$

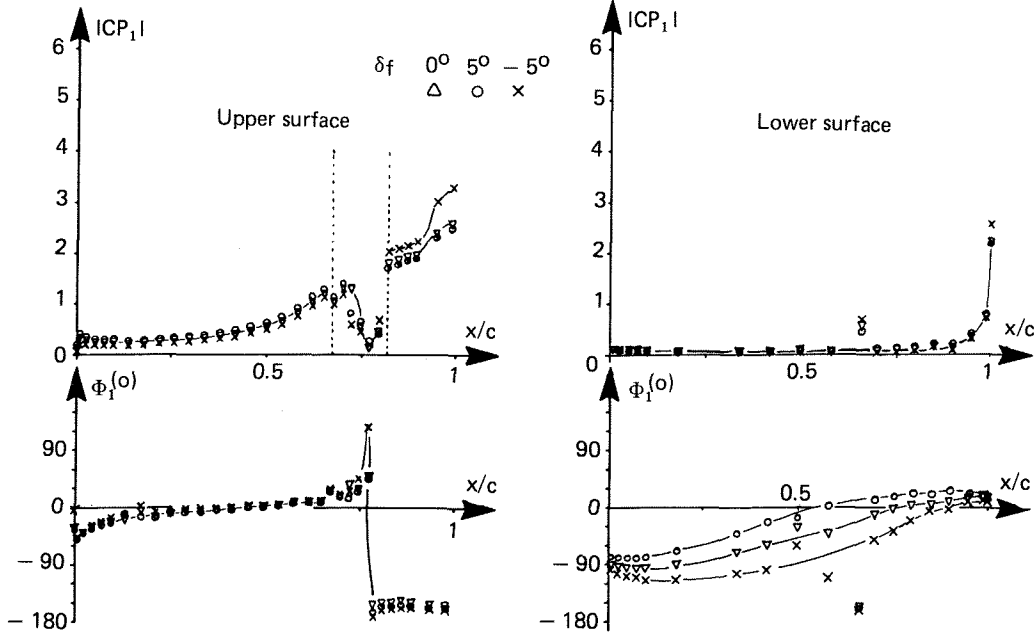


Figure 16. Oscillating spoiler : influence of flap deflection.

b) Flap efficiency versus spoiler deflection

For steady configurations, figure 17 shows that the spoiler mean deflection influences the flap efficiency only for $\delta_{sp} = 5^\circ$, i.e. when the flow behind the spoiler is not fully separated.

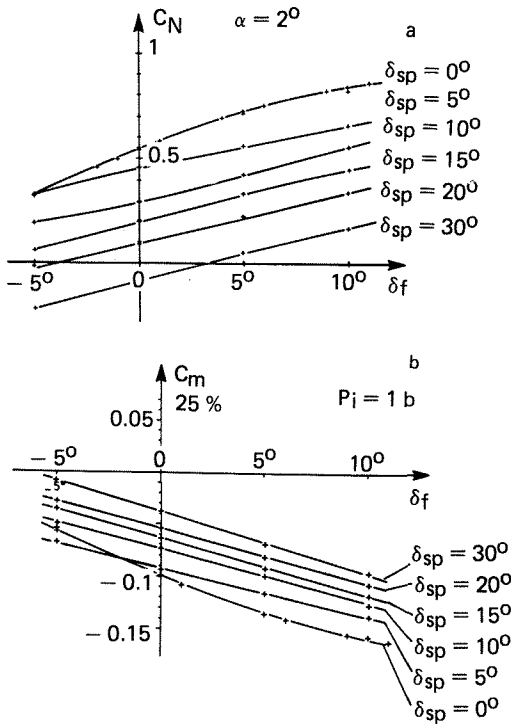


Figure 17. Influence of spoiler deflection on the flap efficiency.

For greater spoiler deflections, the flap moves in a separated flow but the curves $C_N(\delta_{sp})$ and $C_M(\delta_{sp})$ become more linear and the lift and moment curve shapes are the same whatever the spoiler angle may be. This efficiency is, however, lower than in the case without spoiler erected.

For the oscillating flap (figure 18), the unsteady pressure remains quite constant from $\delta_{sp} = 10^\circ$ except on the flap itself. Otherwise, it is not obvious that unsteady pressures must be the same when pure harmonic and white noise excitations are performed on a flap in a separated flow region. A large loss of efficiency as well as a mean phase shift of about 20° appears when the spoiler deflection is increased from 0° to 10° . This point has to be taken into account if active controls are applied to flaps: the gain and phase margins of such controls must be large enough to be stable in all configurations.

V. Ramp type excitation of spoiler and flap

Because spoilers behave nonlinearly, especially for small deflections, additional investigations are necessary for other time history motions representative of flight conditions. Consequently, ramp-like motions represented by

$$\delta(t) = \begin{cases} \delta_0 + \frac{1}{2} (\delta_{max} - \delta_0) (1 - \cos[\pi \frac{t-t_0}{t_1-t_0}]) & t_0 \leq t \leq t_1 \\ \delta_{max} & t_1 \leq t \leq t_2 \\ \delta_0 + \frac{1}{2} (\delta_{max} - \delta_0) (1 + \cos[\pi \frac{t-t_2}{t_3-t_2}]) & t_2 \leq t \leq t_3 \end{cases}$$

have also been used for spoiler and flap excitation. The parameters examined were the

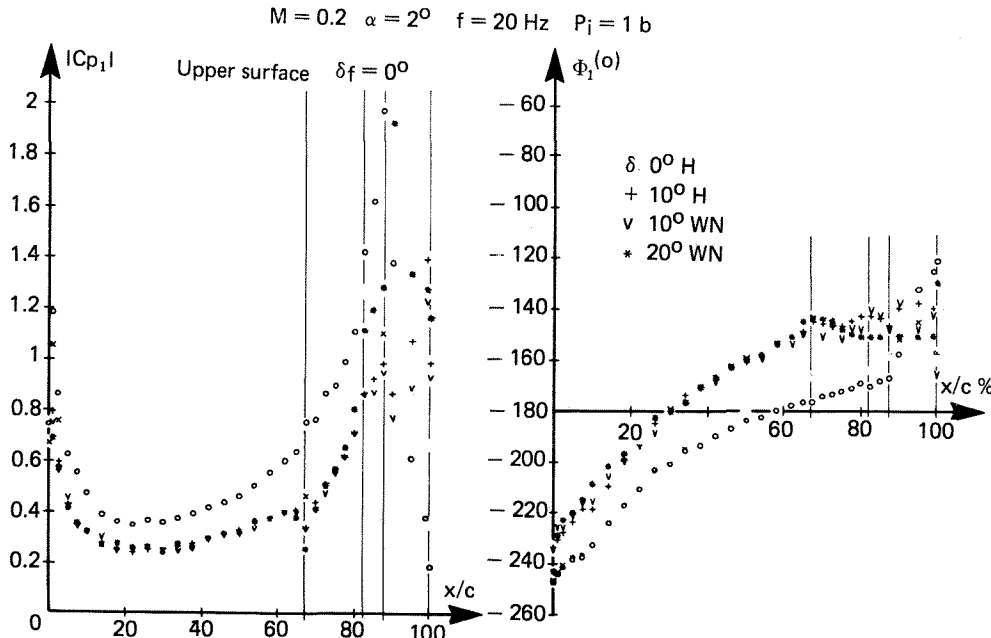


Figure 18. Oscillating flap : influence of spoiler deflection.

starting deflection δ_0 , its maximum value δ_{max} and the deflection rate $\dot{\delta}$. The relation between the time corner points was $(t_1-t_0, t_2-t_1, t_3-t_2) = (1, 2, 1)$.

Figure 19 shows some selected pressure time histories measured on the airfoil for a spoiler ramp motion. The pressure response is nonlinear only on the rear part of the spoiler and behind it, i.e., where separated flows can occur during the spoiler motion. These nonlinearities are larger when the deflection starts from $\delta_0 = 0^\circ$ and they increase with the deflection rate. On the rear part of the spoiler, the pressure at the starting phase gives opposite values compared to static ones. Behind the spoiler, the pressures start also with small opposite values but they turn suddenly into a large overshoot. This behaviour can also be seen below the spoiler for fast motions.

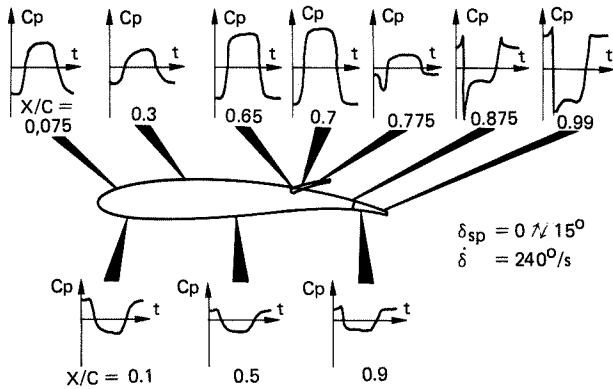


Figure 19. Time history pressure distribution for a spoiler ramp movement.

This adverse behaviour can be seen on the lift and moment coefficients (figure 20.a). The nonlinear effect is more important on the moment coefficient because the nonlinearities mainly appear on the rear part of the airfoil upper surface. A response lag can also be seen for

both coefficients. At last, the adverse effect is smaller when the erection starts with positive spoiler deflections (figure 20.b) or when the deflection rate is getting smaller. In this case, the response lag also decreases.

For a flap ramp motion (figure 21), no adverse effect appears, but a slight overshoot is still present.

VI. Comparison between steady computations and experiment

A computer code based on strong viscous-inviscid interaction has been developed at the ONERA Theoretical Aerodynamics Branch by J.C. Le Balleur². Its ability to take into account strong viscous effects and consequently, separated flows has led to the development of a spoiler application³. The main characteristics of the code are :

- a strong coupling method in direct or semi-inverse mode is assured between the inviscid flow, calculated from the full potential equation written in a conservative form, and the viscous region calculated from integral equations of a defect formulation ;
- the spoiler is modelled by changing the boundary conditions on the airfoil like in small perturbation techniques : the slope at the wall is increased by the spoiler deflection in the spoiler region, and a jump equal to the spoiler height is imposed to the displacement thickness at the spoiler tip.

This code has been used for some configurations tested in the F1 wind tunnel. Figure 22 shows good agreement between computed and measured pressures for $\delta_{sp} = 0^\circ/10^\circ$ for the 2 extreme Reynolds numbers tested. On figure 23, the evolution of the integrated coefficients (lift and moment) versus spoiler deflection for $\delta_f = -5^\circ/0^\circ/5^\circ/10^\circ$ is plotted. The agreement between computed and experimental results is generally good. The region of no efficiency for small spoiler angles is well predicted and its

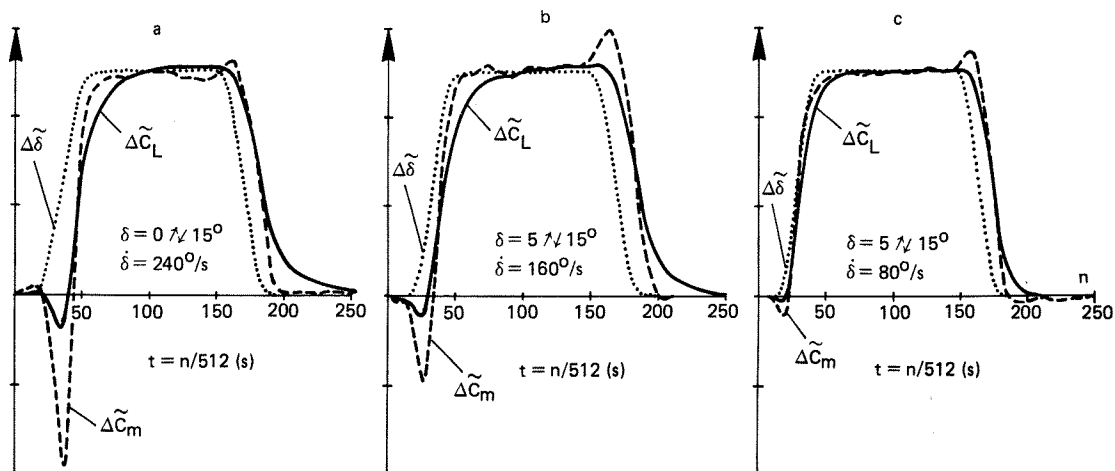


Figure 20. Time histories of normalised increments of spoiler deflection $\Delta\delta$, lift ΔC_L and pitch moment ΔC_m .

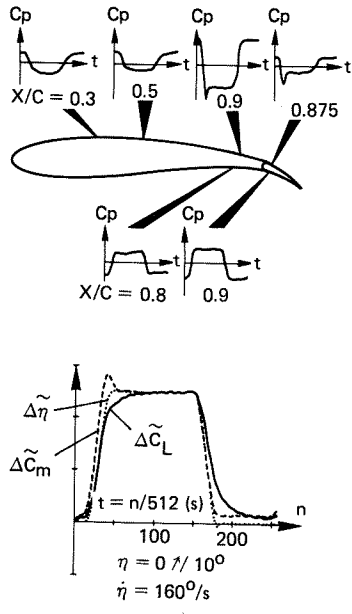


Figure 21. Time histories for pressure distribution and normalised integrated coefficients for a flap ramp movement.

evolution with the flap angle, too. However, in the linear region, the spoiler efficiency is overestimated by the computations. Figure 24 shows a comparison between computed and experimental drag evolution versus spoiler angle. The code which calculates the pressure and skin friction drags also predicts quite well the experimental airfoil drag as measured in the wake.

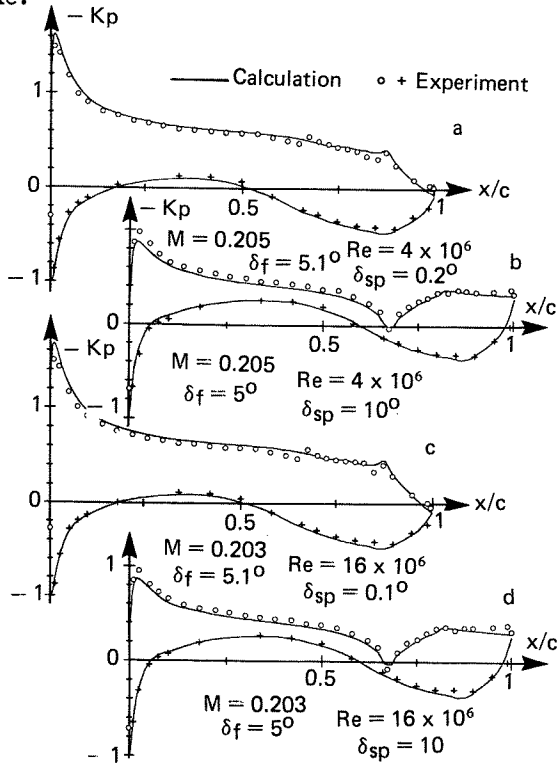


Figure 22. Airfoil with spoiler; comparison calculation-experiment; influence of Reynolds number.

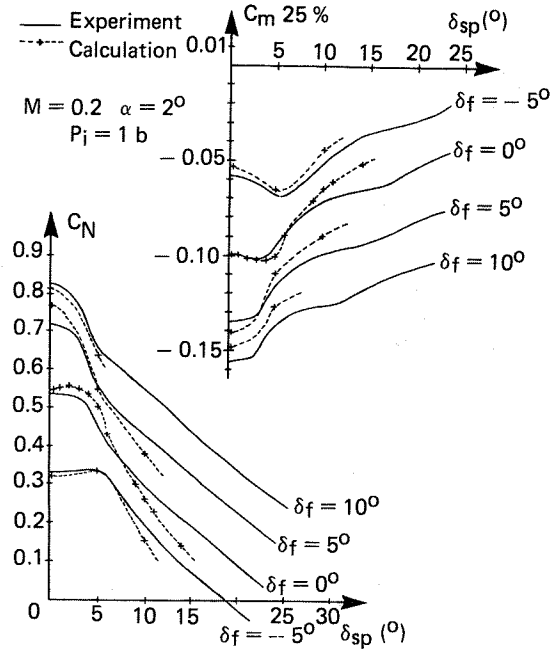


Figure 23. Airfoil with spoiler and flap; comparison calculation-experiment; lift and moment evolutions.

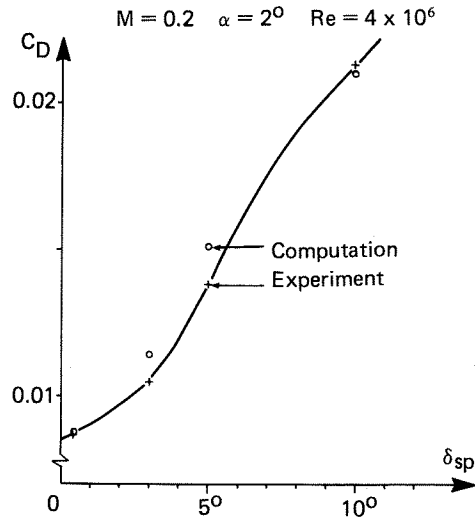


Figure 24. Airfoil with spoiler; comparison calculation-experiment; influence of spoiler deflection on the drag coefficient.

VII. Conclusions

The tests performed on the ACTTA Wing in the ONERA F1 wind tunnel have made it possible to collect numerous and accurate data concerning the steady and unsteady flows around an airfoil equipped with a spoiler and a flap. The results presented here have shown that the Reynolds number effect is very weak for this supercritical airfoil, and, for the unsteady configurations, noticeable only when separated zone fluctuations can be observed on the airfoil (small spoiler angles or/and great flap angles). The examination of spoiler and flap

performances proves that, for this model, the spoiler efficiency can be higher than that of the flap, but with a significant phase lag penalty for the spoiler. It has also been observed that the steady and unsteady performances of spoiler and flap evolve rapidly with their mean static angle when the spoiler angle is small. Because of this important interaction, a great care must be taken in the control design. However, one can hope that these effects are smaller in realistic three-dimensional flows⁴. Finally, ramp measurements have confirmed the much more nonlinear behaviour of the spoilers already observed for harmonic oscillations. Furthermore, they have shown the overshoot phenomena which are specific to these transient movements.

Computational results obtained with a two-dimensional viscous code using a strong coupling technique developed at ONERA have proven the ability of this code to describe the very complex flow appearing when a spoiler is erected.

VIII. References

1. CHRISTOUX, C., GRAVELLE, A., "A digital unit for measuring unsteady pressure coefficients". La Recherche Aéronautique No. 1980-1 (English and French Edition), 1980.
2. LE BALLEUR, J.C., "Strong matching method for computing transonic viscous flows including wakes and separations - Lifting airfoils". La Recherche Aéronautique No. 1981-3, p. 21-45 (English and French Edition), 1981.
3. LE BALLEUR, J.C., "Calculation method for transonic separated flows over airfoils including spoiler effects". Proceedings 8th ICNMF Aachen, Lecture Notes in Physics, Springer-Verlag, June 1982.
4. DESTUYNDER, R., BARREAU, R., ANDERS, G., "Efficiency of different control surfaces in quasi steady and unsteady motion applications". 61th AGARD SMP Meeting - Oberammergau, September 1985.